

Selective Transcutaneous Delivery of Energy to Porcine Soft Tissues Using Intense Ultrasound (IUS)

W. Matthew White, MD,¹ Inder Raj S. Makin, MD, PhD,² Michael H. Slayton, PhD,² Peter G. Barthe, PhD,² and Richard Gliklich, MD^{1*}

¹Division of Facial Plastic and Reconstructive Surgery, Department of Otolaryngology, Massachusetts Eye and Ear Infirmary, Harvard Medical School, Boston, Massachusetts

²Ulthera, Inc., Mesa, Arizona

Objective: Various energy delivery systems have been utilized to treat superficial rhytids in the aging face. The Intense Ultrasound System (IUS) is a novel modality capable of transcutaneously delivering controlled thermal energy at various depths while sparing the overlying tissues. The purpose of this feasibility study was to evaluate the response of porcine tissues to various IUS energy source conditions. Further evaluation was performed of the built-in imaging capabilities of the device.

Materials and Methods: Simulations were performed on ex vivo porcine tissues to estimate the thermal dose distribution in tissues after IUS exposures to determine the unique source settings that would produce thermal injury zones (TIZs) at given depths. Exposures were performed at escalating power settings and different exposure times (in the range of 1–7.6 J) using three IUS handpieces with unique frequencies and focal depths. Ultrasound imaging was performed before and after IUS exposures to detect changes in tissue consistency. Porcine tissues were examined using nitro-blue tetrazolium chloride (NBTC) staining sensitive for thermal lesions, both grossly and histologically. The dimensions and depth of the TIZs were measured from digital photographs and compared.

Results: IUS can reliably achieve discrete, TIZ at various depths within tissue without surface disruption. Changes in the TIZ dimensions and shape were observed as source settings were varied. As the source energy was increased, the thermal lesions became larger by growing proximally towards the tissue surface. Maximum lesion depth closely approximated the pre-set focal depth of a given handpiece. Ultrasound imaging detected well-demarcated TIZ at depths within the porcine muscle tissue.

Conclusion: This study demonstrates the response of porcine tissue to various energy dose levels of Intense Ultrasound. Further study, especially on human facial tissue, is necessary in order to understand the utility of this modality in treating the aging face and potentially, other cosmetic applications. *Lasers Surg. Med.* 40:67–75, 2008. © 2008 Wiley-Liss, Inc.

Key words: nonablative devices; porcine tissue; ex vivo; aging face; collagen; ultrasound; Intense Ultrasound; skin; SMAS; muscle

INTRODUCTION

Ultrasound-based imaging systems for clinical diagnosis have been used for several decades, whereby this energy modality is considered to be one of the safest and used routinely for fetal obstetric and general clinical examinations [1]. However, by using a highly directive source geometry with the source energy settings increased significantly, ultrasound energy can be focused spatially in a tightly confined region (on the order of 1 mm³) to cause selective tissue thermal coagulation (Fig. 1). This Intense Ultrasound (IUS) approach enables the creation of well defined thermal injury zones (TIZs) at depths within soft tissue while leaving the surrounding regions unaffected. IUS is similar to fractional laser resurfacing [2] in that thermal lesions are created, yet IUS is unique in that the thermal lesions are created below the surface and can be of variable geometry. The ultrasound waves induce a vibration in the composite molecules within tissue during propagation, and the friction developed between intrinsic molecules is the source of the generated heat. It has been well established in the literature that Intense Ultrasound (IUS) fields can be transcutaneously directed into visceral soft tissue to produce coagulative necrosis resulting primarily from thermal mechanisms [3,4]. For most of the work in this area, the effort has been to develop intense focused ultrasound as a noninvasive surgical tool to treat human whole organ tumors, such as liver, breast, and uterus [3,4].

In order to achieve an effective energy delivery for cosmetic applications, a novel ultrasound therapy device is described herein to deposit energy localized to the first few

Presented in part at the April 2006 Annual Meeting of the American Society of Lasers in Surgery and Medicine in Boston, MA.

Contract grant sponsor: Ulthera, Inc., Mesa, AZ.

The authors have disclosed potential financial conflict of interests with this study.

*Correspondence to: Richard Gliklich, MD, Division of Facial Plastic and Reconstructive Surgery, Massachusetts Eye and Ear Infirmary, 243 Charles Street, Boston, MA 02114.

E-mail: richard_gliklich@meei.harvard.edu

Accepted 27 December 2007

Published online in Wiley InterScience
(www.interscience.wiley.com).

DOI 10.1002/lsm.20613

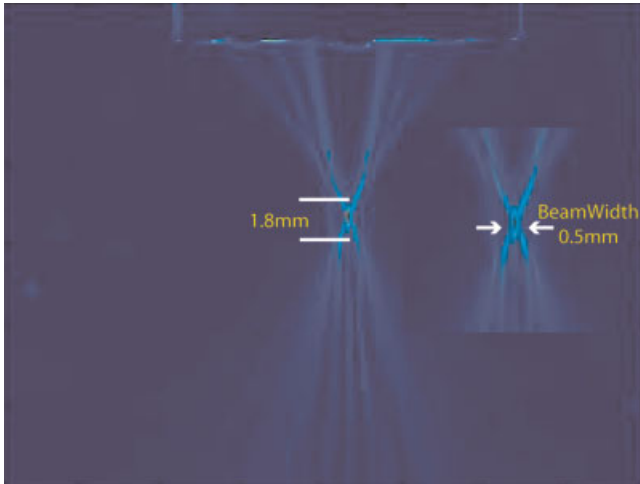


Fig. 1. Intense Ultrasound beam profile. Visualization of an ultrasound beam using a Schlieren system enables the mapping of the power density (Intensity) of the field [22,23]. The Schlieren map of one of the prototype probes used in this study demonstrates that most of the ultrasound energy (approximately 95% of total energy), can be focused spatially into a tightly confined region. As shown in this result, the focal zone of the ultrasound beam was measured to be 1.8 mm axially, while the beam was 0.5 mm in the radial direction (inset: magnified view of focal region). [Figure can be viewed in color online via www.interscience.wiley.com.]

millimeters of the superficial skin tissue [5,6]. This device is able to focus energy within tissue to produce a 25 mm line of discrete TIZs spaced 0.5–5.0 mm apart. Furthermore, both imaging and selective energy exposure can be accomplished with the same handpiece. The IUS System can therefore target and deliver focused energy to a specific soft tissue region or layer.

Various nonsurgical modalities have been utilized to treat facial rhytids (peels, microdermabrasion, and lasers) [7,8]. All of these modalities however have focused on treating the superficial layers of skin (i.e., epidermis and dermis) due to their limited penetration depth. The gold standard for nonsurgical facial rejuvenation has been the Carbon Dioxide (CO₂) Laser. The CO₂ laser has been used extensively for facial resurfacing for the treatment of rhytids. The mechanism of CO₂ laser rejuvenation of the skin is thought to be: (i) ablating and removing the most superficial layer of skin (epidermis), and (ii) delivering energy to the deeper superficial papillary dermis to create a lesion in the collagen [9–12]. This lesion incites a “wound healing” response through the liberation of several cytokines which stimulate fibroblasts to synthesize and lay down new collagen. This collagen remodeling process is a crucial step in facial skin rejuvenation.

Despite the efficacy of the CO₂ laser, treatment results in complete ablation of the entire epidermis with a wound that lasts for 7–10 days. Following this, post-treatment erythema or “scalded skin” appearance that can persist for months after CO₂ laser resurfacing. Although CO₂ laser

resurfacing has been proven largely successful for the nonsurgical treatment of rhytids, the undesirable post-operative intense inflammatory response has caused the demand for this procedure to drop dramatically. For this reason, physicians and surgeons alike have tried to develop various methods (e.g., radiofrequency), termed “Nonablative Skin Resurfacing,” to induce collagen shrinkage and remodeling while preserving the epidermis in an effort to minimize these post-operative changes. These modalities have produced variable efficacy at best [7,8,13].

In this initial study, we wanted to determine if the IUS system could be used to create subsurface, discrete TIZs. Porcine tissue was used since it is a well-established model in terms of tissue properties being close to that of human skin [10,11,14]. Numerical modeling was first performed to simulate IUS energy–tissue interaction. Homogeneous porcine muscle tissue was then utilized to examine the dose–response profile by varying unique source conditions of the IUS system (e.g., frequency, time, source power). Lesions were measured, quantified and compared with the theoretical predictions. Ultrasound imaging was performed before and after IUS exposure to determine if TIZ localization was possible. A subset of the energy dose range from experiments conducted in porcine muscle was then repeated in porcine skin tissue using the three IUS handpieces. This work serves as an introductory feasibility study investigating superficial tissue response to IUS exposure.

MATERIALS AND METHODS

Fresh, frozen specimens of porcine muscle and skin were obtained according to the policies of the Massachusetts Eye and Ear Infirmary Institutional Review Board (IRB). Specimens were stored in a freezer, and allowed to thaw to room temperature (25°C) prior to experiments.

Intense Ultrasound System

The IUS device is designed to target and deliver focused ultrasound energy within tissue (Ulthera, Inc., Mesa, AZ). The IUS handpiece contains a transducer that has two functioning modes: imaging (which is used to image the region of interest before the therapeutic ultrasound exposures) and treatment (which is the mode that delivers a series of higher-energy ultrasound exposures). A series of selective thermal ablative zones can be produced along a straight line at a given depth within the tissue (25 mm line of discrete lesions spaced 0.5–5.0 mm apart). For each series of exposures, the following source conditions can be varied: power output (W), exposure time (ms), length of exposure line (mm), distance between exposure zones (mm), and time delay after each exposure (ms). Three handpieces were used, in order of most superficial focus to the deepest: (i) 7.5 MHz 3 mm focal depth, (ii) 7.5 MHz 4.5 mm focal depth, and (iii) 4.4 MHz 4.5 mm focal depth in tissue.

Numerical Simulations

The acoustic field and the resulting thermal distribution in tissue resulting from absorption of the focused beam were simulated numerically for each of the three handpieces.

The thermal effects of a focused field propagating through skin/superficial tissue have been extensively modeled using well-established acoustic beam propagation schemes [13–16] as well as using the bio-heat equation [15–18]. A multi-layer approach has been applied for numerical simulations, whereby the significant differences in tissue attenuation between the epidermis (nominal thickness 0.2 mm), dermis, and subcutaneous tissue have been accounted for. The 60°C temperature contour in tissue is representative of the region with thermal coagulation within the source conditions used in this study.

IUS Exposure Procedure

The porcine skin tissue was tattooed (India ink) prior to IUS exposures to create a grid over the proposed treatment area (Fig. 8). Porcine muscle specimens were first selected. A range of source conditions were selected and planned for each area. Prior to each treatment, ultrasound imaging of the soft tissue was performed to identify the target tissues. Ultrasound imaging was performed on each planned treatment area and still images were captured and stored. All IUS exposures were performed along the parallel axis of the tattooed grid. Immediately after IUS exposure lines were delivered, the handpiece was left in place and the axis of the

exposure line delivered was marked by the use of Wite-Out[®] Correction Fluid (Bic Corporation, Milford, CT; Fig. 8).

After all IUS exposures for a given porcine specimen had been completed, each treated region was excised. The tissue bloc was then placed on an acrylic plate and kept in a –15 degree Celsius freezer for approximately 2 hours. Using a surgical blade, fine 1 mm thick sections were cut parallel to the IUS exposure lines. In the case of the porcine muscle experiments, the zones of thermal coagulation are revealed as discrete whitened regions. These slices are photographed and the digital images assessed in terms of the size and shape of the thermal zone.

For porcine skin experiments, the grossly sectioned thin strips of skin tissue was placed in NBTC stain overnight for viability staining. This method has been described in the literature for identifying thermally affected tissue both in vivo as well as for ex vivo studies [19–21]. Viable tissue stains blue and TIZs are demarcated by a pale color or lack of blue staining. Digital photographs (Nikon D-70, Nikon USA, Melville, NY) were taken of the gross tissue sections after they NBTC staining. Depth and dimensions of TIZ were evaluated from digital photographs of post-NBTC-stained gross porcine tissue strips using image processing software (NIH Image J, <http://rsbweb.nih.gov/ij/>).

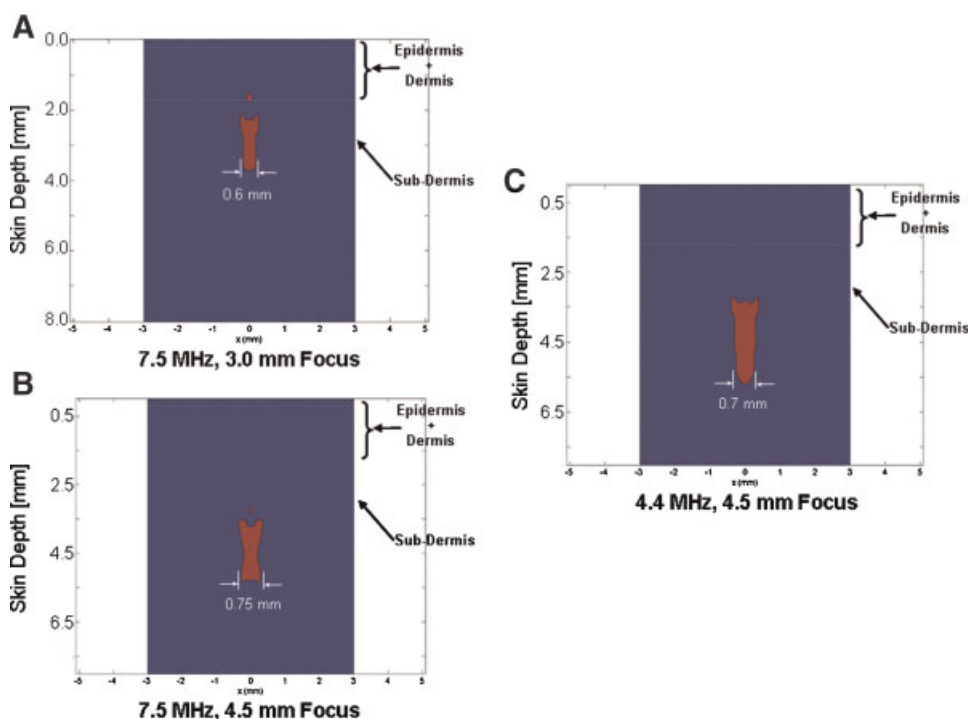


Fig. 2. IUS simulation. Numerical simulation of the thermal response of porcine skin tissue to a focused Intense Ultrasound beam. The epidermis and dermis is modeled as a single layer of higher attenuation (2.0 dB/MHz/cm), compared to the subdermal tissue (1.5 dB/MHz/cm). Irreversible tissue coagulation is represented in these numerical simulations as the region of porcine skin tissue that attains a temperature $\geq 60^\circ\text{C}$ using one

of the three handpieces. The y-axis represents the depth (millimeters) from the probe–tissue interface. The x-axis is the width (millimeters) of the TIZ. **A:** 7.5 MHz/3.0 mm focus probe, **B:** 7.5 MHz/4.5 mm focus probe, and **C:** 4.4 MHz/4.5 mm focus probe. [Figure can be viewed in color online via www.interscience.wiley.com.]

RESULTS

Numerical Simulations

Multiple simulation runs were performed to predict the zone of thermal coagulation in porcine muscle as well as skin tissue. Representative results for the three handpiece configurations used in this study are shown in Figure 2. These simulations represent propagation through porcine skin tissue. The simulations predict a spatially confined zone of thermal treatment within the tissue. The numerically predicted results (Fig. 2) compare favorably with regions of tissue coagulation demonstrated in gross tissue specimens (Fig. 9).

Porcine Muscle

Porcine muscle was chosen for the initial experimentation due to its homogeneous composition. In this experiment, an IUS probe with a source frequency of 4.4 MHz and focal depth of 4.5 mm was chosen. Exposure lines were delivered to porcine muscle specimens as power levels were increased. Visual analysis of porcine tissue revealed that as the source power was increased from 2.3 to 7.6 J, the TIZ became larger and extended closer to the tissue surface (Fig. 3). For lower source settings (2.3 J), the thermal injury region is relatively small and corresponds closely to the geometric focal zone of the ultrasound field. As the energy of the IUS source is increased (2.3–7.6 J), the initial tissue coagulation at the focus presents a region of significantly higher acoustic attenuative characteristics, thereby “screening” the thermal injury region from extending post-focally. The TIZ then progressively extends proximally towards the Intense Ultrasound source plane.

Figure 4 shows a series of exposures using the 7.5 and 4.4 MHz (4.5 mm focal depth) handpieces. Lesion locations and dimensions were measured and were observed to be dependent on particular source conditions such as

source frequency, focal depth, power, and exposure duration (energy). Imaging scans were made immediately pre- and post-exposure in each case. The images in each case, demonstrate a selective hyper-echogenic string of regions, which correspond reasonably well with the grossly visualized TIZs.

In order to better characterize the tissue effect, the proximal and distal range of the TIZ as well as the corresponding areas are quantified for each exposure condition. Analysis of these tissue samples shows a dose–response effect of tissue ablation with source conditions for the 7.5 MHz (Fig. 5) and 4.4 MHz (Fig. 6) handpieces. For both the sources, the proximal edge of the TIZ progressively extends upwards with increasing source energy, and the lesion becomes larger (greater area).

Porcine Skin

Porcine skin is considered a reasonable model for investigating the effect for energy for cosmetic applications [9,10]. Figure 7 shows histologic demonstration of TIZs from an *in vivo* experiment utilizing the 7.5 MHz 4.5 mm focal depth probe. Figure 7A shows an image of a hematoxylin and eosin stain (H&E) slide, whereas the Figure 7B shows a gross section of the skin sample stained with vital stain (NBTC). Both the images are captured at 10× magnification. The source conditions for the IUS-treated regions in both samples are the same. Note that the nominal depth and dimensions of the TIZs identified in both the separate skin samples were created using the same source conditions, yet compare favorably when evaluated by different staining techniques (Fig. 7). The hematoxylin and eosin staining example shows a region of selective and distinct thermal coagulative change, where the collagen fibers are indistinct and fused together, whereas the loss of vital staining (nitro-blue tetrazolium chloride—NBTC) within the region of the TIZ indicates

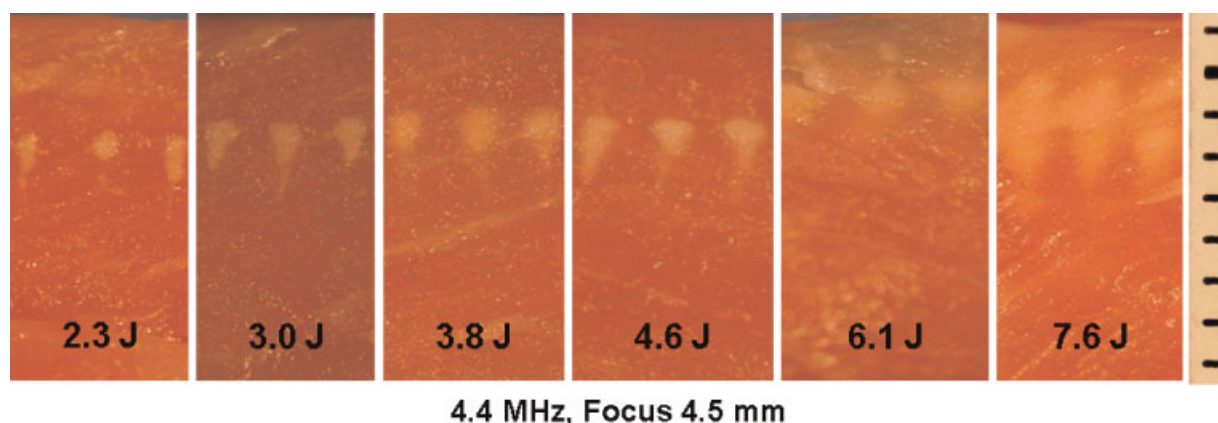


Fig. 3. Dose–response in muscle. Digital photographs of gross tissue sections (approximately 1 mm thick) of porcine muscle reveal profile of changes in geometry of TIZ as the source energy is increased from 2.3 to 7.6 J. Within the homogeneous orange-colored muscle tissue, the white inverse-pyramidal regions of coagulated tissue are the TIZs resulting from the ultrasound exposure (4.4 MHz, 4.5 mm focus handpiece). [Figure can be viewed in color online via www.interscience.wiley.com.]

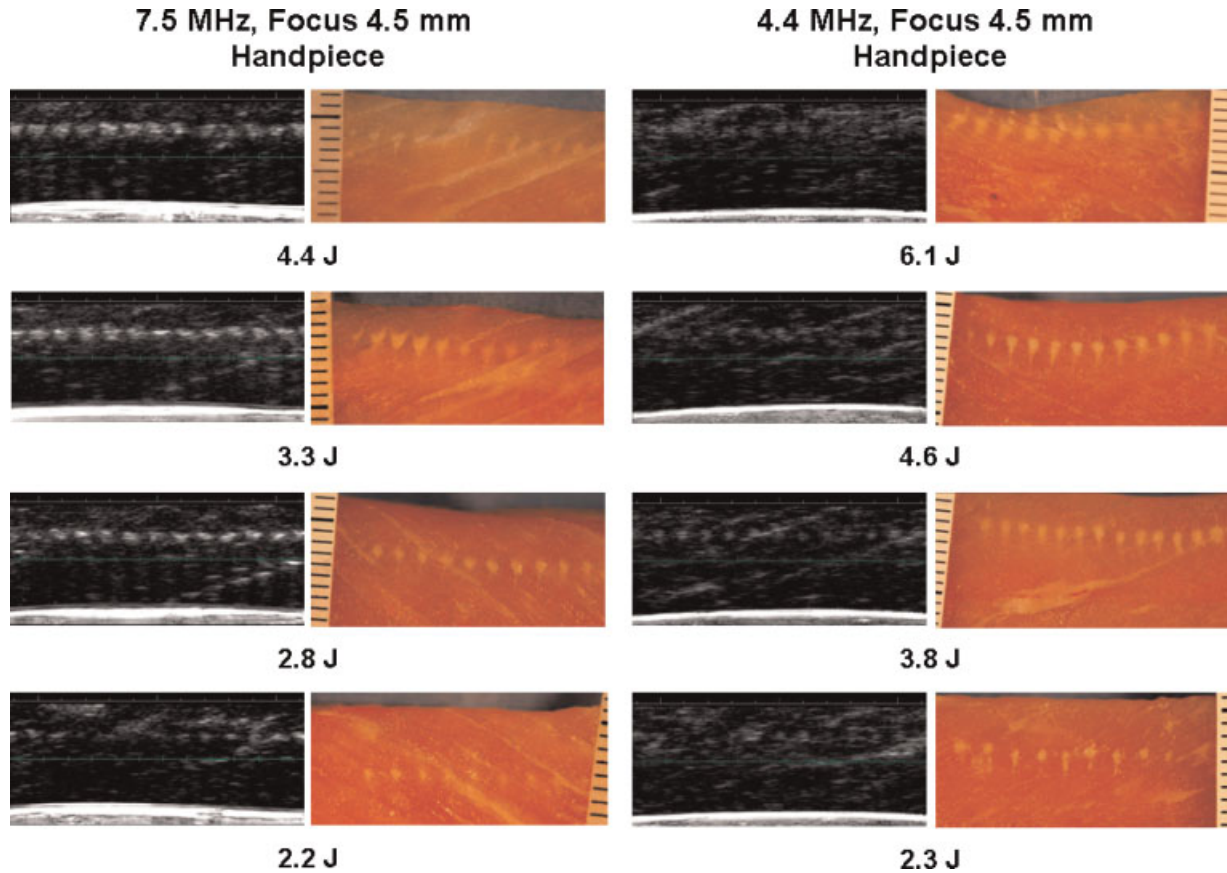


Fig. 4. Image guided therapy—ultrasound imaging of TIZ. Geometry of the TIZs over different source conditions could be viewed with the integrated ultrasound imaging modality of two IUS handpieces. Both ultrasound images and digital photographs of gross tissue sections (1 mm thick) of porcine muscle are shown. [Figure can be viewed in color online via www.interscience.wiley.com.]

thermal denaturation. No damage to the skin surface was observed in this *in vivo* porcine experiment.

In Figure 9, a series of representative results are shown in gross tissue sections using each of the three handpieces investigated in this study. The three handpieces help achieve TIZ depth and shape unique to the probe geometry (3.0 or 4.5 mm focal depth) as well as source frequency (7.5 or 4.4 MHz). As predicted in the numerical simulations (Fig. 2), the 7.5 MHz handpiece with 4.5 mm focal depth results in a TIZ that is nominally shallower with a shorter axial dimension compared to the TIZ from the 4.4 MHz (4.5 mm focus) handpiece. This observation is confirmed by comparing the axial range of TIZs in Figure 9B,C. Note that in each case (Fig. 9A–C), the epidermal layer is spared. As described in the Materials and Methods Section, multiple TIZs were placed along a 25 mm exposure line at each source condition using a particular handpiece. Figure 8 shows that the porcine skin surface after placing two exposure lines each, for the three probes using the energy settings from Figure 9. No skin surface damage was observed during exposure with either of the three handpieces.

DISCUSSION

In this work, we introduce a new approach that has the potential for use in facial cosmetic procedures. We have shown that IUS is capable of creating thermal coagulative zones at depths within porcine soft tissues. Trials with different handpieces demonstrate that for the same source geometry (e.g., 7.5 vs. 4.4 MHz probes with 4.5 mm focal depth), lower frequency exposures tend to produce TIZs that extend deeper within tissue (compare Figs. 5 and 6). The results in Figures 5 and 6 respectively, have a low variability and demonstrate creation of well controlled TIZs at each source condition.

The tissue response characterized by thermal coagulation change, achieved by IUS exposure is similar to that from other energy-based devices used in the cosmetic arena such as lasers, radiofrequency (RF) and combination laser–RF devices [9,10,19]. However, in contrast to the other known energy based devices used for cosmetic applications, the IUS field is sharply focused, thereby depositing most of the energy in the form of heat around the focal zone of the beam, leaving the surrounding regions

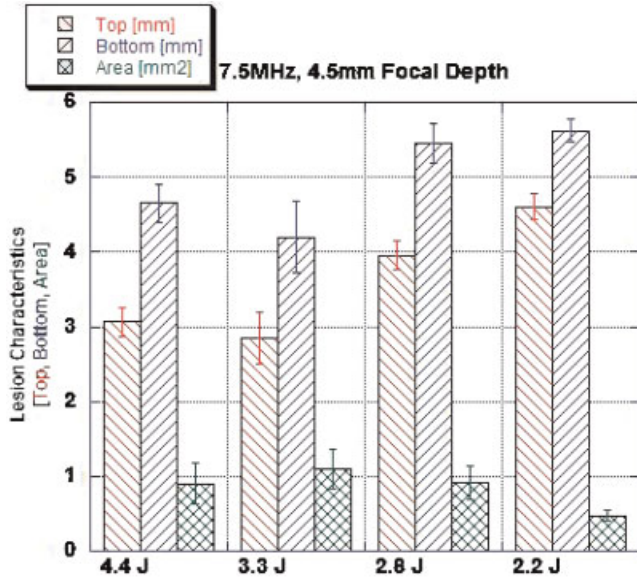


Fig. 5. Graph of coagulative zone characteristics with the 7.5 MHz, 4.5 mm handpiece. Effect of varying source condition on the size and depth of the TIZs ($N=39$). The red bars represent the average measurement of the most superficial portion (labeled “Top”), of the TIZs from the surface of the sample tissue. The blue bar is the average measurement of the deepest portion of the TIZs from the tissue surface (labeled “Bottom”). The Green bar is the average estimated area of the TIZs at various source settings. Each error bar corresponds to one standard deviation for each measurement. [Figure can be viewed in color online via www.interscience.wiley.com.]

unaffected [3,4]. In this manner, the overlying epidermal surface is spared, and the thermal coagulation is achieved only at depth (on the order of millimeters). The hypothesis is that this approach of selective thermal injury at depth will avoid unwanted side effects seen with ablative skin resurfacing modalities (e.g., skin pigmentary change and sloughing).

The primary biophysical processes leading to thermal coagulation during propagation of ultrasound energy as considered in this investigation are: beam focusing and acoustic absorption. In the case of a tightly focused beam, the maximum rate of acoustic energy deposition in the form of heat is around the focal plane. The remaining pre-focal and post-focal areas of the beam in tissue remain unaffected, since the acoustic power density is insufficient to achieve thermal tissue coagulation in regions other than the focal zone (Figs. 3, 7, and 9). Acoustic absorption is a frequency dependent phenomenon, nominally increasing linearly with frequency in tissue [14]. Therefore, the 4.4 MHz handpiece (4.5 mm focal depth), tends to achieve a TIZ deeper compared to the 7.5 MHz (4.5 mm focus) handpiece (Figs. 2 and 9).

In this study, porcine tissue was chosen as for experiments, since it is an established tissue model for cosmetic tissue applications [9,10,20]. For example, porcine skin

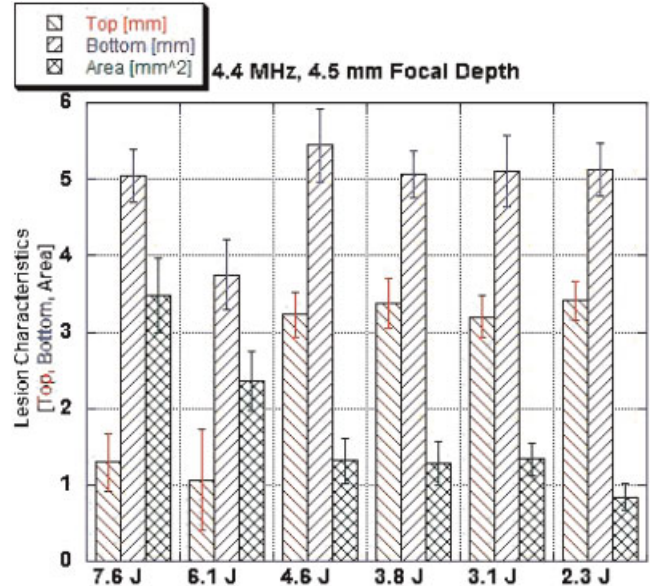


Fig. 6. Graph of TIZ characteristics with the 4.4 MHz, 4.5 mm handpiece. Effect of varying source condition on the size and depth of the TIZs ($N=73$). The red and blue bars represent the proximal (“top”) and distal (“bottom”) extents of the TIZ. Green bar is the average area of the TIZs at a particular source setting. [Figure can be viewed in color online via www.interscience.wiley.com.]

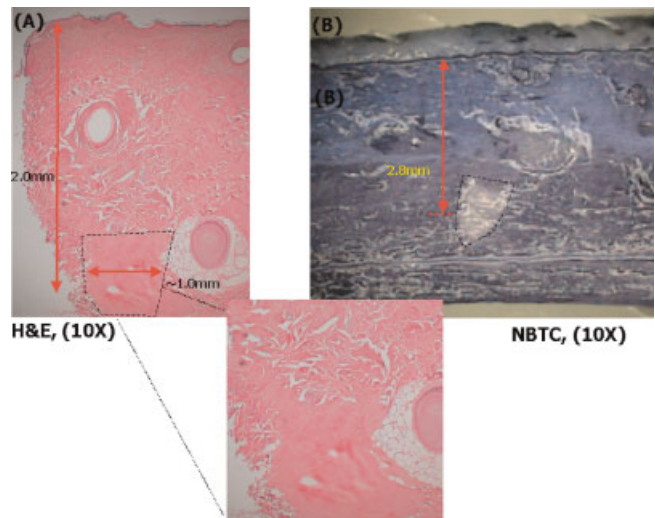


Fig. 7. Thermal coagulative region with the 7.5 MHz, 4.5 mm focal depth handpiece (3.6 J). Comparison of thermal coagulative change with H&E (histology) and NBTC staining of a gross tissue section of porcine skin (both figures in vivo treatment). Note homogenization of the collagen fibrillar structure with hematoxylin and eosin staining (A), and thermal damage in a comparable zone (no blue-dye uptake) with NBTC staining (B). The inset panel shows a magnified view of the coagulation zone using H&E staining. [Figure can be viewed in color online via www.interscience.wiley.com.]

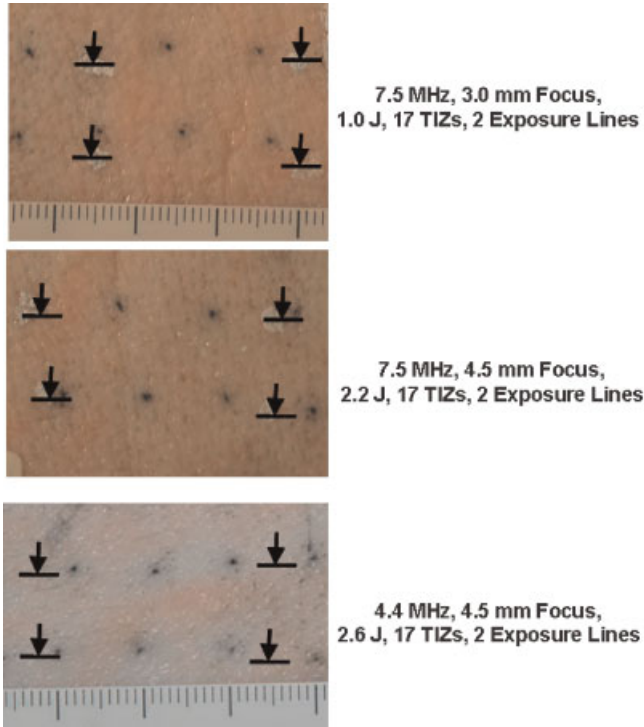


Fig. 8. Skin surface after exposure with 7.5 MHz, (3.0 and 4.5 mm focal depths) and 4.4 MHz, 4.5 mm focal depth handpieces. Note no damage to skin surface after placement of multiple TIZs along two exposure lines using each handpiece. The vertical arrows indicate the borders of a single exposure line. Photographs were taken prior to sectioning and staining to observe TIZs in skin tissue in Figure 9. [Figure can be viewed in color online via www.interscience.wiley.com.]

has a similar layered structure as human skin: epidermis, dermis and glandular components, underlying connective tissue and muscle. Even though the attenuation coefficient of porcine muscle is much lower than skin tissue (muscle, 0.75 dB/MHz/cm compared to skin, 2.0 dB/MHz/cm) [14], the porcine muscle tissue is used as a model to understand the energy–tissue interaction and reliably demonstrate selective thermal coagulation using a focused IUS beam. Using porcine muscle, a wide range of source parameters could be varied and the tissue effect could be easily evaluated with gross pathology as regions of whitened coagulum, even without NBTC staining (Figs. 3 and 4). As described earlier, increasing the energy levels significantly resulted in propagation of the TIZ towards the surface (Figs. 3 and 5). This phenomenon of “tadpole formation” is well documented in the literature for other soft tissue ablation with IUS [20]. Therefore, the degree of selectivity of tissue effect in skin can be controlled by an appropriate choice of source conditions for a particular handpiece.

In the case of porcine skin tissue, the various anatomical layers, epidermis, dermis and subcutaneous tissue are represented. The regions of thermal coagulative necrosis identified using NBTC staining are representative of

the TIZs expected in the human facial skin tissue. The numerical simulation results for formation of thermal lesions in a porcine skin tissue, accounting for attenuation and focusing (Fig. 2) are comparable to the actual porcine skin experimental results (Fig. 9). A key goal of this concept study was to understand the characteristics of selective thermal coagulation using Intense Ultrasound in model tissue (porcine muscle, and porcine skin—in vitro and in vivo). Tissue contraction following ultrasound exposure was not investigated since the tissue was not attached to the natural anatomical attachment points, and will be the subject of future studies.

Ultrasound imaging is unique to the IUS device in that it could potentially provide immediate feedback to the clinician. In these initial experiments, we demonstrated that it is possible to detect the thermal coagulative change that occurs in porcine muscle tissue following IUS exposure (Fig. 4). However, detecting TIZ in porcine skin tissue by ultrasound imaging was more challenging. Imaging the lesion size and location can represent added safety to the clinician, as it is possible to see immediately where the energy is being deposited. Further work needs to be performed in optimizing the ultrasound imaging component of the system, and in understanding the role of imaging in developing an IUS based cosmetic procedure.

The mechanism of skin rejuvenation has been well studied in the gold standard CO₂ laser. The CO₂ laser has a dramatic “skin tightening effect” which is routinely observed by clinicians immediately after the delivery of laser pulses [8–11]. The mechanism of skin tightening is a heat induced denaturation of the collagen fibers facilitated by disruption of collagen cross-linking bonds that results in an immediate shrinkage. It has been well demonstrated in the literature that thermal induced shrinkage of collagen by various devices repeatedly occurs when connective tissue is heated to 65–75°C [6–10]. The IUS approach offers a potential for a similar thermal tissue effect at depth, with the exception that the detrimental effects of epidermal disruption can be avoided. Further investigative work must be focused on the ultrastructural effect of IUS based collagen denaturation, the degree of tissue shrinkage produced by different IUS energy doses, and the safety of this device in treating human patients.

CONCLUSION

This report demonstrates the creation of discrete TIZs in porcine muscle and skin specimens using Intense Ultrasound energy. We have tested the response of these tissue models over a broad range of energy doses. We were able to demonstrate a dose range that produces selective, well-circumscribed TIZs at a desired depth (e.g., dermis or subcutaneous tissues), without overlying epidermal disruption. Thermal induced collagen denaturation is an integral step in skin tightening by various laser and radiofrequency devices. These energy modalities are however, either depth-limited or energy density limited to achieve selective thermal coagulation deep within the skin tissue. Using ultrasound energy, this work is a

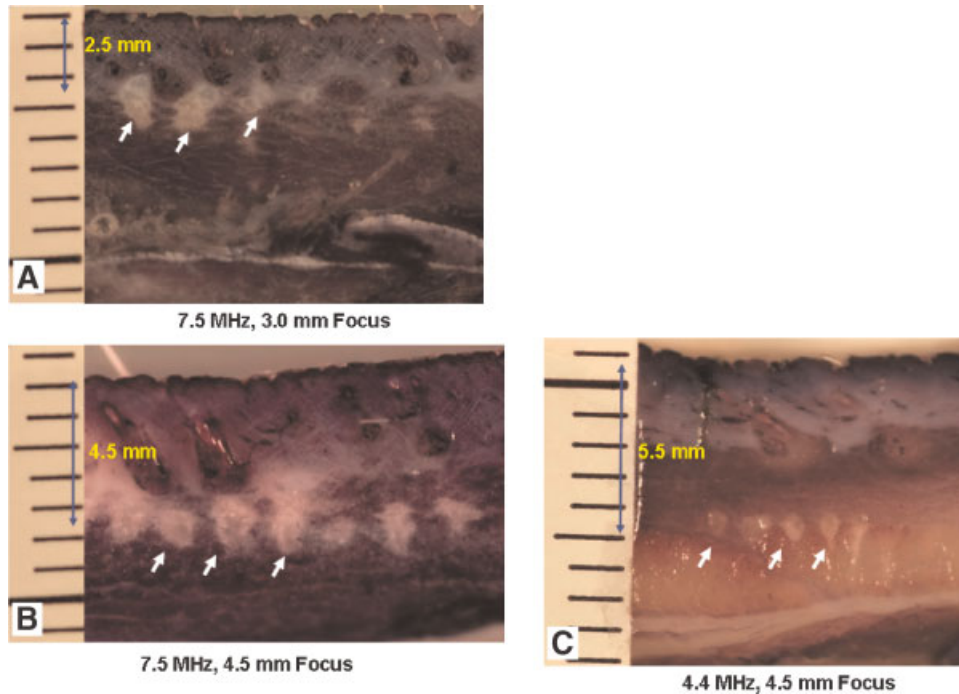


Fig. 9. NBTC stained gross tissue sections of porcine skin. The lesion profile of these three different IUS handpieces demonstrates variability in thermal injury zones (arrows), as the dermis and underlying tissue is targeted. Note that the TIZs resulting from the 7.5 MHz, 4.5 mm focus handpiece (10B) extends nominally shallower compared to the TIZs from the 4.4 MHz, 4.5 mm focus handpiece (10C). **A:** 7.5 MHz, 3.0 mm focus (1 J); **B:** 7.5 MHz, 4.5 mm focus (2.2 J); and **C:** 4.4 MHz, 4.5 mm focus (2.6 J). [Figure can be viewed in color online via www.interscience.wiley.com.]

demonstration of the ability to create controlled thermal coagulative zones at various depths (order of millimeters), within skin tissue, targeting respective anatomical layers, while sparing the overlying epidermis. It is also possible with the IUS device to detect TIZs with the built-in ultrasound imaging component of the device.

The range of selective TIZs demonstrated using Intense Ultrasound in this study extends from the dermis up to the level of subcutaneous structures of the facial skin tissue. The potential for using this device in treating the aging face is encouraging, and needs to be investigated further in human tissues [24–26].

ACKNOWLEDGMENTS

Funding for this work was provided in part by the Ulthera, Inc., Mesa, AZ.

REFERENCES

- McGahan JP, Goldberg BB, editors. *Diagnostic ultrasound: A logical approach*. Wickford: Lippincott-Raven; 1997.
- Manstein D, Herron GS, Sink RK, Tanner H, Anderson RR. Fractional photothermolysis: A new concept for cutaneous remodeling using microscopic patterns of thermal injury. *Lasers Surg Med* 2004;34:426–438.
- Kennedy JE, ter Haar GR, Cranston D. High intensity focused ultrasound: Surgery of the future? *Br J Radiol* 2003;76:590–599.
- Makin IRS, Mast TDM, Faidi WF, Runk MM, Barthe PG, Slayton MH. Miniaturized arrays for interstitial ablation and imaging. *Ultrasound Med Biol* 2005;31(11):1539–1550.
- Laubach H-J, Barthe PG, Makin IRS, Slayton MH, Manstein D. Confined thermal damage with Intense Ultrasound (IUS). *Laser Surg Med* 2006;38(18):32.
- White WM, Makin IRS, Barthe PG, Slayton MH, Gliklich RE. Selective transcutaneous delivery of energy to facial subdermal tissues using the ultrasound therapy system. *Laser Surg Med* 2006;38(18):87.
- Hruza GJ. Rejuvenating the aging face. *Arch Facial Plast Surg* 2004;6:366–369.
- Kim KH, Geronemus RG. Nonablative laser and light therapies for skin rejuvenation. *Arch Facial Plast Surg* 2004;6:398–409.
- Kirsh KM, Zelickson BD, Zachary CB, Tope WD. Ultrastructure of collagen thermally denatured by microsecond domain pulsed carbon dioxide laser. *Arch Dermatol* 1998;134:1255–1259.
- Ross EV, Naseef GS, McKinlay JR, Barnette DJ, Skrobal M, Grevelink J, Anderson RR. Comparison of carbon dioxide laser, erbium:YAG laser, dermabrasion, and dermatome. A study of thermal damage, wound contraction, and wound healing in a live pig model: Implications for skin resurfacing. *J Am Acad Dermatol* 2000;42:92–105.
- Ross EV, Yashar SS, Naseef GS, Barnette DJ, Skrobal M, Grevelink J, Anderson RR. A pilot study of in vivo immediate tissue contraction with CO₂ skin resurfacing in a live farm pig. *Dermatol Surg* 1999;25:851–856.
- Goco PE, Stucker FJ. Subdermal carbon dioxide laser cutaneous contraction. *Arch Facial Plast Surg* 2002;6:37–40.
- Zelickson BD, Kist D, Bernstein E, Brown DB, Ksenzenko S, Burns J, Kilmer S, Mehregan D, Pope K. Histology and

- ultrastructural evaluation of the effects of a radiofrequency-based nonablative dermal remodeling device. *Arch Dermatol* 2004;140:204–209.
14. Goss SA, Johnston RL, Dunn F. Comprehensive compilation of empirical ultrasonic properties of mammalian tissues. *J Acoust Soc Am* 1978;64:423–457.
 15. Hasegawa T, Matsuzawa K, Inoue N. *J Acoust Soc Am* 1986;79(4):927–931.
 16. Nyborg WL. Heat generation by ultrasound in a relaxing medium. *J Acoust Soc Am* 1981;70:310–312.
 17. Mast TDM, Makin IRS, Faidi WF, Runk MM, Barthe PG, Slayton MH. Bulk ablation of soft tissue with intense ultrasound: Modeling and experiments. *J Acoust Soc Am* 2005;118(4):2715–2724.
 18. Mast TD, Faidi WF, Makin IRS. Acoustic field modeling in therapeutic ultrasound. *Intl Symp Nonlinear Acoust* 2005; 17th International Symposium on Nonlinear Acoustics, State College PA, AIP Conference Proceedings 838, edited by A.A. Atchley, V.W. Sparrow, and R.M. Keolian (American Institute of Physics, New York, 2005): 209–216.
 19. Neumann RA, Knobler RM, Pieczkowski F, Gebhart W. Enzyme histochemical analysis of cell viability after argon laser-induced coagulation necrosis of the skin. *J Am Acad Dermatol* 1991;25(6 Part I):991–998.
 20. Misbah HK, Sink RK, Manstein D, Eimerl D, Anderson RR. Intradermally focused infrared laser pulses: Thermal effects at defined tissue depths. *Laser Surg Med* 2005;36:270–280.
 21. Anderson RR, Farinelli W, Laubach H, Manstein D, Yaroslavsky AN, Gubeli III J, Jordan K, Neil GR, Shinn M, Chandler W, Williams GP, Benson SV, Douglas DR, Dylla HF. Selective photothermolysis of lipid-rich tissues: A free electron laser study. *Laser Surg Med* 2006;38:913–919.
 22. Sadick NS, Trelles MA. Nonablative wrinkle treatment of the face and neck using a combined diode laser and radiofrequency technology. *Dermatol Surg* 2005;31:1695–1699.
 23. Watkin NA, ter Haar GR, Rivens I. The intensity dependence of the site of maximal energy deposition in focused ultrasound surgery. *Ultrasound Med Biol* 1996;22(4):483–491.
 24. Dierickx CC. The role of deep heating for noninvasive skin rejuvenation. *Laser Surg Med* 2006;38:799–807.
 25. White WM, Makin IR, Barthe PG, Slayton MH, Gliklich RE. Selective creation of thermal injury zones in the superficial musculoaponeurotic system using intense ultrasound therapy: a new target for noninvasive facial rejuvenation. *Arch Facial Plast Surg*. 2007;9(1):22–29.
 26. Gliklich RE, White WM, Slayton MH, Barthe PG, Makin IR. Clinical pilot study of intense ultrasound therapy to deep dermal facial skin and subcutaneous tissues. *Arch Facial Plast Surg*. 2007;9(2):88–95.